Supplementary Material for

Tetrameric structure of GlfT2 reveals a scaffold for the assembly of mycobacterial arabinogalactan

Robert W. Wheatley,[1,2] Ruixiang Blake Zheng,[1,3] Michele R. Richards,[1,3]
Todd L. Lowary*,[1,3] and Kenneth K. S. Ng*,[1,2]

[1]Alberta Glycomics Centre
[2]Department of Biological Sciences University of Calgary, Calgary AB, T2N 1N4, Canada
[3]Department of Chemistry, Gunning-Lemieux Chemistry Centre University of Alberta,
Edmonton AB, T6G 2G2, Canada

Email: ngk@ucalgary.ca, tlowary@ualberta.ca

SUPPLEMENTARY TABLE 1.

Oligonucleotide Primer Sequences Used for Site-Directed Mutagenesis

E300S	Sense	GCCATCTGCACATCATGGGTTCAGTTGTCGACCGTTCTA
	Antisense	TAGAACGGTCGACAACTGAACCCATGATGTGCAGATGGC
D371S	Sense	GCCGCTGTTTATTAAATGGAGCGATGCCGATTATGGTCTG
	Antisense	CAGACCATAATCGGCATCGCTCCATTTAATAAACAGCGGC
D372S	Sense	CGCTGTTTATTAAATGGGACTCTGCCGATTATGGTCTGCGTG
	Antisense	CACGCAGACCATAATCGGCAGAGTCCCATTTAATAAACAGCG
W399S	Sense	CTGGCACATGGCGTCGTCTGACAAAGACG
	Antisense	CGTCTTTGTCAGACGACGCCATGTGCCAG
H413S	Sense	GATGCAATTGATTGGCAGGCTTATTTTTCTCTGCGTAACCGCC
	Antisense	GGCGGTTACGCAGAGAAAAATAAGCCTGCCAATCAATTGCATC

SUPPLEMENTARY FIGURE LEGENDS

Supplementary Figure 1. Topology diagram of GlfT2 showing how secondary structure elements in different domains (colored as in Fig. 1) are connected to each other. Residue numbers for secondary structure elements are given in the table at right.

Supplementary Figure 2. Schematic diagram showing conserved residues in different domains forming inter-domain interactions. The numbers in blue indicate the %-age of sequences showing either perfect identity (or in a few cases identity among a few related residue types, as noted) in an alignment of 150 of the unique sequences currently found in the non-redundant subset of Genbank and aligned using CLUSTALW [1].

Supplementary Figure 3. Hypothetical model of UDP-Gal*f* (red) and β-D-Gal*f*-(1→5)-β-D-Gal*f*-(1→4)-α-L-Rha*p*-(1→3)-α-D-Glc*p*NAc-decaprenyl-pyrophosphate bound to the GlfT2 tetramer, with domains for subunit 1 colored as in Fig. 1. Different parts of the lipid-linked acceptor are colored as follows: Gal*f* residues magenta, Rha and GlcNAc cyan, pyrophosphate orange and decaprenol black. The approximate location of the junction between the hydrophilic and hydrophobic portions of the membrane is denoted by blue spheres, as calculated by the PPM server [2]. (A) Stereoscopic view of the model with GlfT2 drawn in a semi-transparent surface representation. (B) Semi-transparent cartoon representation of GlfT2. The side chains of exposed hydrophobic and positively charged residues in domains 3 and 4 of GlfT2 are drawn in stick representation and labeled.

Supplementary Movie 1. Animation in which an electrostatic surface representation of the unliganded GlfT2 tetramer is rotated between the N-face, side and C-face views.

Supplementary Movie 2. Animation in which a semi-transparent electrostatic surface representation of the GlfT2 tetramer bound to models of UDP-Gal*f* (green spheres) and a lipid-linked tetrasaccharide (Gal*f* disaccharide colored magenta, Rha-GlcNAc disaccharide colored cyan, pyrophosphate colored orange and decaprenol colored black) acceptor is rotated between the N-face, side and C-face views.

REFERENCES

1. Larkin, M.A. et al. Clustal W and Clustal X version 2.0. *Bioinformatics* 23, 2947-8 (2007).
2. Lomize, M.A., Pogozheva, I.D., Joo, H., Mosberg, H.I. & Lomize, A.L. OPM database and PPM web server: resources for positioning of proteins in membranes. *Nucleic Acids Res.* 40, D370-6 (2012).

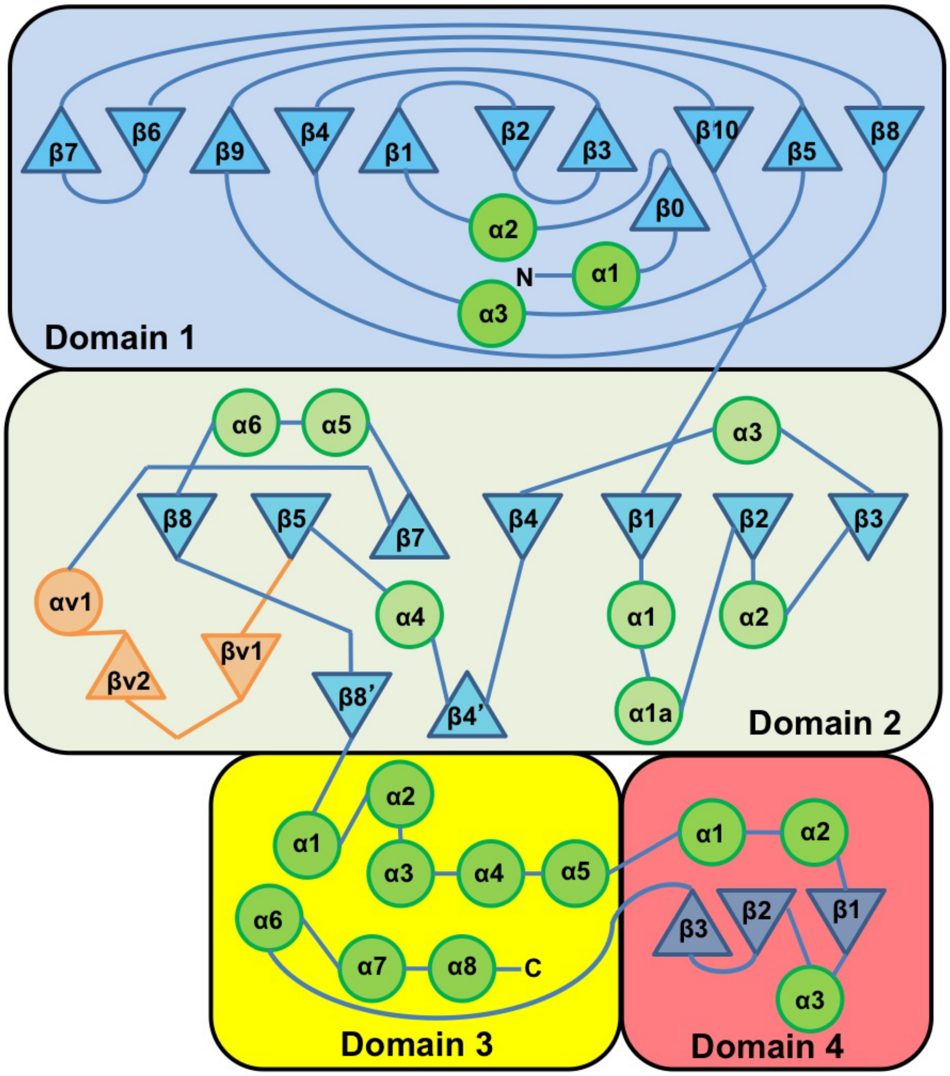

Domain 1		Domain 2	
α1	2-6	β1	162-165
β0	8-11	α1	172-182
α2	21-25	α1a	186-190
β1	29-30	β2	192-199
β2	39-42	α2	210-218
β3	45-48	β3	222-226
β4	52-55	α3	230-246
α3	65-71	β4	251-254
β5	76-84	β4'	259-261
β6	88-94	α4	263-275
β7	100-110	β5	281-288
β8	116-123	βv1	294-297
β9	132-139	βv2	300-303
β10	143-151	αv1	331-337
		β7	350-353
		α5	354-360
		α6	371-382
		β8	386-390
Domain 3		β8'	392-396
α1	408-423		
α2	431-449	**Domain 4**	
α3	452-467	α1	518-532
α4	469-475	α2	538-542
α5	478-488	β1	546-548
α6	581-600	α3	555-559
α7	602-616	β2	563-567
α8	619-626	β3	574-578

Supplementary Figure 1

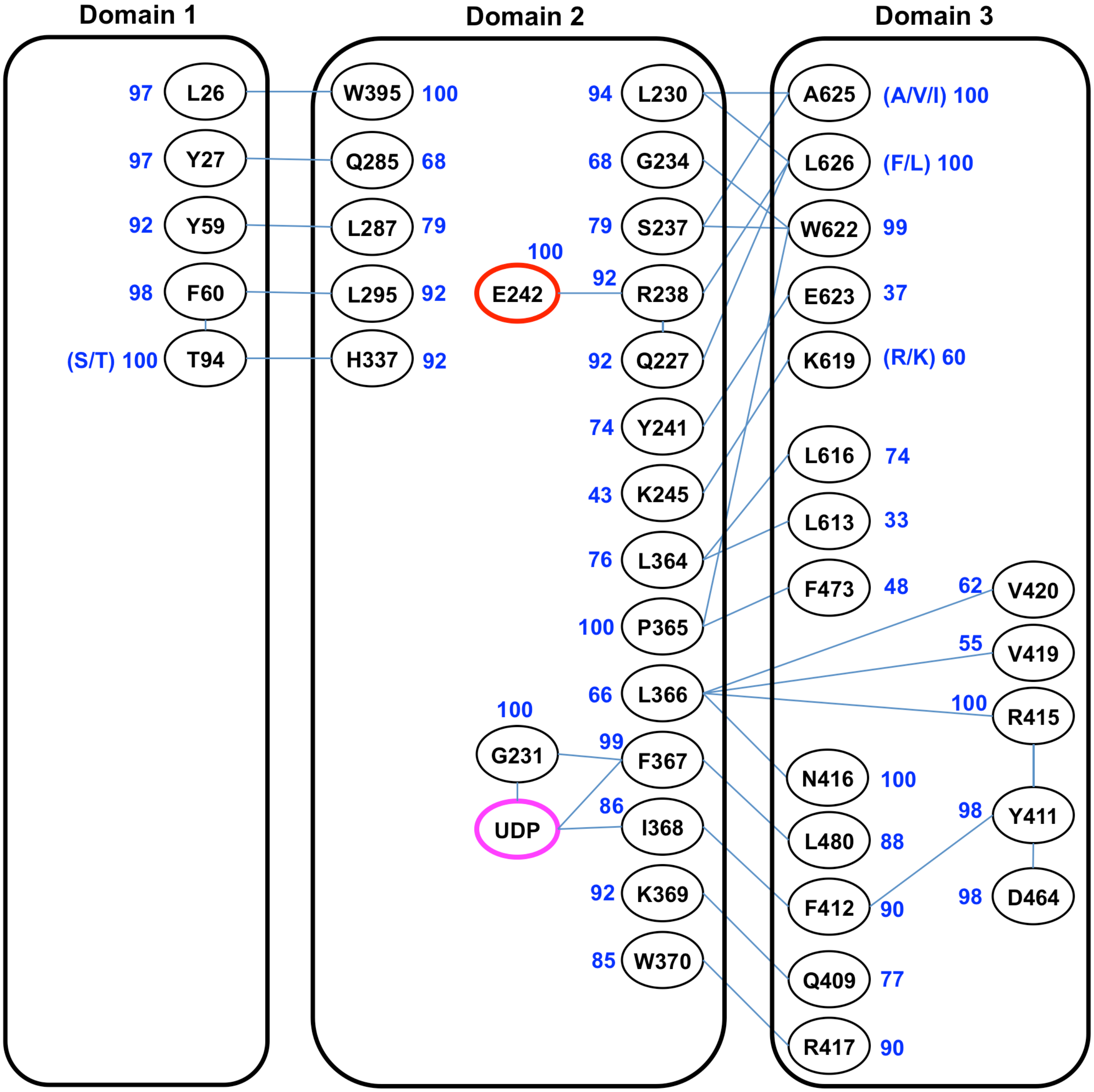

Supplementary Figure 2

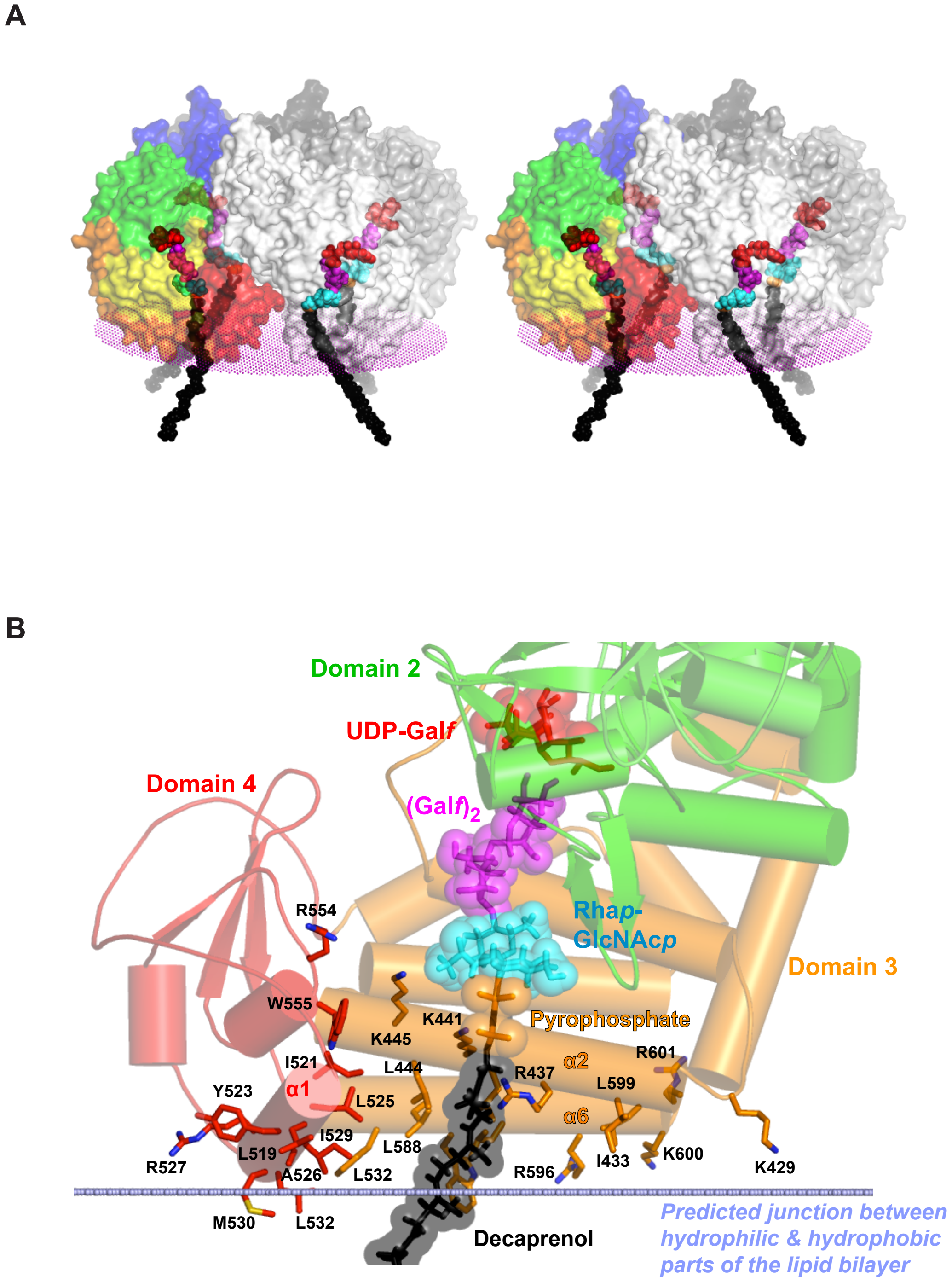

Supplementary Figure 3